Prospects for doubling the range of Advanced LIGO

Prospects for doubling the range of Advanced LIGO

John Miller,* Lisa Barsotti, Salvatore Vitale, Peter Fritschel, and Matthew Evans
LIGO Laboratory, Massachusetts Institute of Technology, 185 Albany Street, Cambridge, Massachusetts 02139, USA

Daniel Sigg
LIGO Hanford Observatory, P.O. Box 159, Richland, Washington 99352, USA
(Received 29 October 2014; published 16 March 2015)

In the coming years, the gravitational-wave community will be optimizing detector performance to target a variety of astrophysical sources which make competing demands on detector sensitivity in different frequency bands. In this paper we describe a number of technologies that are being developed as anticipated upgrades to the Advanced LIGO detectors and quantify the potential sensitivity improvement they offer. Specifically, we consider squeezed light injection for the reduction of quantum noise, detector design and materials changes which mitigate thermal noise and mirrors with significantly increased mass. We explore how each of these technologies impacts the detection of the most promising gravitational-wave sources and suggest an effective progression of upgrades which culminates in a twofold improvement in broadband sensitivity.

DOI: 10.1103/PhysRevD.91.062005 PACS numbers: 04.80.Nn, 07.60.Ly, 95.55.Ym, 95.85.Sz

I. INTRODUCTION

A worldwide network of ground-based gravitational-wave detectors [1–3] promises to begin the era of gravitational-wave astronomy by detecting ripples in space-time produced by astrophysical sources such as coalescing binary neutron stars (BNS) and binary black holes (BBH). These kilometer-scale Michelson-style interferometers are designed to detect gravitational-wave strain amplitudes of 10^{-23} or smaller.

While Advanced LIGO and other advanced detectors are expected to observe tens of compact binary coalescence (CBC) events per year [4], great benefit can be gained by further extending their astrophysical reach [5,6]. This is particularly true for Bayesian studies which combine evidence from multiple detections. For example, it has been shown that gravitational-wave signals recorded by Advanced LIGO can be used to perform strong-field tests of general relativity [7–9] and measure the equation of state of neutron stars [10–12]. Improved sensitivity would lead to more frequent detections, allowing more powerful tests to be performed. A larger catalogue of CBC data would also facilitate study of the distribution of neutron star and black hole masses. Such information enables one to comment on the maximum possible neutron star mass and probe the existence of a mass gap between black holes and neutron stars [13]. Finally, more regular observation of BNS events increases the probability of identifying an electromagnetic counterpart, which may be used to, amongst other things, determine the Hubble constant [14] (although we note that cosmological parameters can be estimated with gravitational-waves alone [15,16]).

In addition to yielding more frequent detections, improving the sensitivity of Advanced LIGO also increases the likelihood of witnessing rare sources. For instance, the existence of intermediate mass black holes [$M \sim \mathcal{O}(10^2–10^3)M_{\odot}$] is still controversial [17]. A single detection would provide the first direct proof of their existence, whereas multiple detections could be used to constraint their formation rate and test the no-hair theorem [18].

Five- to tenfold strain sensitivity improvements are possible but can only be achieved by significantly modifying core components of the existing interferometers [19], by constructing a new ultra–high-vacuum envelope to accommodate longer interferometer arms [20] or both [21]. In this paper we analyze a progression of upgrades to Advanced LIGO which do not require changes to the current buildings or vacuum infrastructure and, as much as possible, leverage proven technologies. While such upgrades have previously been discussed in isolation, here we examine realistic combinations of these upgrades and provide a coherent strategy and timeline for their implementation. We find that, in combination, these upgrades achieve a factor of two broadband sensitivity improvement. This translates into a detection rate increase approaching one order of magnitude.

II. SENSITIVITY IMPROVEMENT TARGETS

Quantum noise and thermal noise are the principal fundamental noise sources in Advanced LIGO (see Fig. 1). Quantum noise is produced by shot noise, the

*jmiller@ligo.mit.edu

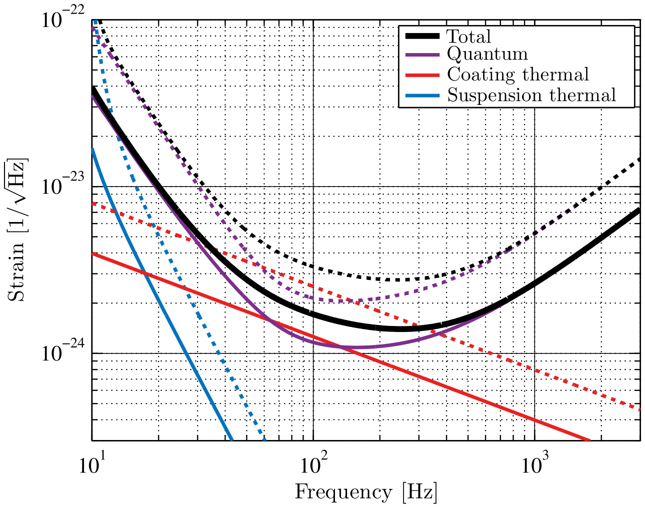

FIG. 1 (color online). Strain sensitivity of a possible upgraded Advanced LIGO interferometer. Improved thermal noise (factor of two), improved quantum noise (16 m filter cavity and 6 dB of measured squeezing at high frequency) and heavier test masses (also a factor of two) are assumed. The equivalent Advanced LIGO curves are shown using dashed lines.

statistical fluctuations in the arrival time of photons at the interferometer output, and by radiation pressure noise, the fluctuations in the number of photons impinging on the test masses [22,23].

Thermal noise may be explained by the fluctuation-dissipation theorem, which connects displacement fluctuations in a system surrounded by a thermal bath with dissipation caused by internal losses [24]. The dominant sources of thermal noise in current interferometric gravitational-wave detectors are the high-reflectivity optical coatings on the test masses (coating thermal noise) and the fused-silica fibers which suspend the test masses against the force of Earth's gravity (suspension thermal noise) [25].

Squeezed light injection is a proven technique to reduce quantum noise. New lower-loss coating materials or the current optimized amorphous coatings in combination with a larger beam size on the test masses could reduce coating thermal noise by a factor of two or more. Two other possible improvements are considered here: the reduction of suspension thermal noise, which contributes to the total noise below 50 Hz, and a set of heavier test masses, which reduces the impact of radiation pressure noise in the same frequency band.

Figure 1 shows the resulting quantum noise and thermal noise after implementation of all of the improvements discussed in the previous paragraph.

The canonical figure of merit describing the sensitivity of a detector is its range. In this work we define the average BNS range to be $\sqrt[3]{3/64 \times 1.8375} \simeq 1/2.26$ times the redshift-corrected luminosity distance at which an optimally oriented and located BNS system consisting of two $1.4M_\odot$ neutron stars would give a matched-filter signal-to-noise ratio of 8 in a single detector [26–28]. We also consider the analogous BBH range for a system consisting of two $10M_\odot$ black holes. The baseline Advanced LIGO interferometers should each achieve a BNS range of up to 220 Mpc and a BBH range of up to 1.3 Gpc.

TABLE I. BNS and BBH ranges for an Advanced LIGO interferometer in which combinations of the main limiting noise sources have been reduced in the manner described in the text. A plausible incremental progression of upgrades is highlighted in blue: (i) quantum noise reduction through squeezed light injection, (ii) a factor of two reduction in coating thermal noise, (iii) a factor of two increase in the mirror mass and (iv) a factor of two reduction in suspension thermal noise.

	Improved quantity				Range	
	Quantum	Coating thermal	Mirror mass	Suspension thermal	BNS [Mpc]	BBH [Gpc]
	—	—	—	—	220	1.3
(i)	•	—	—	—	280	1.5
	—	•	—	—	280	1.7
	—	—	•	—	260	1.6
	—	—	—	•	220	1.3
(ii)	•	•	—	—	400	2.3
	•	—	•	—	320	1.9
	•	—	—	•	280	1.6
	—	•	•	—	350	2.3
	—	•	—	•	280	1.7
	—	—	•	•	270	1.7
(iii)	•	•	•	—	470	2.9
	•	•	—	•	410	2.3
	•	—	•	•	320	1.9
	—	•	•	•	350	2.3
(iv)	•	•	•	•	480	3.0

Note that, in these and other computations, we focus on noise sources driven by fundamental physical processes, acknowledging that, in common with all previous generations of interferometer, technical and non-Gaussian noise must be mitigated before fundamental noise sources are exposed.

Table I shows how subsets of the improvements affect the detector's range. No single improvement guarantees more than a 30% increase in range with respect to Advanced LIGO. However, once combined, the range can be approximately doubled. The status and prospects of these technologies are described in the following sections.

III. SQUEEZED LIGHT FOR QUANTUM NOISE REDUCTION

Squeezed states of light [29] have already been employed to improve the sensitivity of gravitational-wave interferometers [30,31] and are routinely used in GEO600 [32]. However, any reduction in quantum shot noise at high frequencies is accompanied by a commensurate increase in

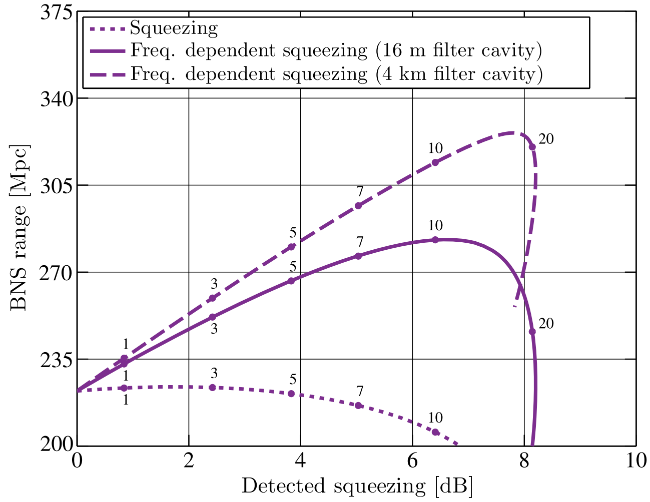

FIG. 2 (color online). Impact of squeezing in Advanced LIGO on BNS range as a function of measured high-frequency quantum noise reduction. Numerical labels indicate the magnitude of squeezing injected in dB. The best experimentally detected level currently stands at approximately 12 dB [33]. A longer filter cavity does not significantly improve the effectiveness of squeezing in Advanced LIGO.

quantum radiation pressure noise. If applied to Advanced LIGO, squeezing would reshape the sensitivity of the detector as a function of frequency to the detriment of BNS range (see Fig. 2).

By reflecting a squeezed state from a detuned high-finesse optical resonator, known as a filter cavity, one can produce frequency dependent squeezing which simultaneously reduces shot noise at high frequencies and radiation pressure noise at low frequencies [34,35].

Interferometers measure the projection of the quantum noise ellipse onto the gravitational-wave signal (see e.g. Fig. 5 of [34]). Technical effects can cause the relative orientation of the ellipse to oscillate as a function of time (phase noise) or introduce noise from the orthogonal axis of the ellipse (mode matching errors, filter cavity loss), coupling antisqueezing into the measurement quadrature and reducing the level of observed squeezing [36]. Increasing the level of squeezing increases the eccentricity of the quantum noise ellipse, making one more susceptible to technical noise of this kind. Thus, more squeezing can lead to reduced sensitivity, as evidenced by the curious double-valued nature of the frequency dependent squeezing curves in Fig. 2.

With a realistic implementation of frequency dependent squeezing (see parameters in Table II and methods described in [36]), broadband improvements are available, leading to increases of 30% and 15% in BNS and BBH ranges, respectively, and valuable improvements in our ability to extract gravitational-wave signal parameters for astrophysical investigations [37].

With 10 dB of injected squeezing, realistic loss mechanisms, mainly the filter cavity intracavity loss, limit the

TABLE II. Parameters used in evaluating the performance of an Advanced LIGO interferometer incorporating frequency dependent squeezing. Interferometer parameters are as given in Table I of [36]. Values in parentheses correspond to an interferometer with 80 kg mirrors.

Parameter	Value
Filter cavity length	16 m
Filter cavity input mirror transmissivity	67(47) ppm
Filter cavity detuning	49(35) Hz
Filter cavity half-bandwidth	56(41) Hz
Filter cavity losses	8 ppm
Injection losses	5%
Readout losses	5%
Mode mismatch (squeezer-filter cavity)	2%
Mode mismatch (squeezer-interferometer)	5%
Frequency independent phase noise (root mean square)	5 mrad
Filter cavity length noise (root mean square)	0.3 pm
Injected squeezing	9.1 dB

range achievable with a 16 m filter cavity to 280 Mpc. A longer filter cavity can mitigate the impact of intracavity losses, as it allows the required storage time (which is fixed by the interferometer) to be achieved with a lower number of cavity round-trips. But, as shown in Fig. 2, even a 4-km-long cavity would only yield a 10% improvement. For this reason, a 16–20 m filter cavity is the baseline option for upgrading Advanced LIGO [38]. To date, frequency dependent squeezing has only been demonstrated at radio frequencies [39]. The research to transfer this technique to gravitational-wave frequencies is ongoing [36,40].

IV. INCREASED MIRROR MASS

Radiation pressure noise scales inversely with the core optics' mass, providing a means of mitigating its impact. The test masses in Advanced LIGO are made from ultralow absorption fused silica. This material is available in sizes allowing for up to about twice the present mass. We thus establish 80 kg as the fiducial mass of our upgraded mirrors. Such an increase demands new suspensions capable of supporting a greater load. However, this can be achieved by mimicking the current suspension design, with straightforward enlargement of springs, fibers and mass elements. The existing seismic isolation system can accommodate the increased mass without modification.

Larger masses should allow the use of larger beams, leading to lower coating thermal noise. From this standpoint, the optimal mirror aspect ratio (radius/thickness) is approximately unity. With such a geometry, coating thermal noise amplitude scales as $m^{-1/3}$, where m is the mirror mass, if the diffraction loss is held constant. Increased mass also reduces suspension thermal noise. This effect scales as $m^{-1/4}$ in amplitude [25] and has been included in the values presented in this work.

V. COATING THERMAL NOISE REDUCTION

The optical coatings used in gravitational-wave detectors have extraordinary optical properties: absorption below 1 ppm, scatter losses around 10 ppm and very tightly controlled reflectivities. Conversely, these coatings are mechanically much more lossy than the mirror substrates on which they are deposited. Thus, they constitute the dominant source of thermal noise [41].

Coating research has received considerable attention in the past decade as the use of resonant optical cavities has become widespread in frequency standards, gravitational-wave detectors and other precision optical measurements [42]. Informed by this work, the coatings used in Advanced LIGO are composed of alternating layers of amorphous silica and titania-doped tantalum pentoxide [43,44]. Despite ongoing research, amorphous materials offering lower losses while maintaining acceptable optical properties have proven elusive [45]. This has led to a search for new coating materials and technologies for use in future gravitational-wave detectors [46].

One potential solution is the use of crystalline coatings. A leading candidate is epitaxial layers of $Al_xGa_{1-x}As$, where the parameter x takes two values to provide the high and low refractive index materials of a multilayer Bragg reflector [47]. Such mirrors can be grown on a GaAs wafer and then transferred to a fused-silica substrate and have been shown to provide at least a factor of three reduction in the amplitude of coating thermal noise [48]. While crystalline coatings are promising, they have yet to be demonstrated on a 50-cm-scale mirror. Scaling up this technology presents several technical challenges, both in the manufacturing process and in meeting the extremely stringent surface-figure specifications associated with multikilometer resonant cavities.

VI. LARGER BEAMS

Increasing the size of the laser beam reflected from the test masses reduces the impact of coating thermal noise in proportion to the beam diameter, simply due to averaging over a larger coating area [42]. While this solution is conceptually simple, feasible beam diameters are limited by optic size, optical stability considerations in the arm cavities and challenges in fabricating suitable mirror surfaces. In the context of Advanced LIGO and current coating technology, even with larger mirrors, no more than a factor of two reduction in coating thermal noise is likely to be achieved without compromising the performance of the interferometer—either due to clipping losses on the optics or angular instabilities in the interferometer [50,51].

Given the potential difficulties associated with new coating materials and larger beam spot sizes it is not certain that either will achieve its estimated performance on the appropriate timescale (~5 years). We therefore expect that a combination of the two approaches will be implemented in order to combat coating thermal noise and that they will provide an improvement of no more than a factor of two.

VII. SUSPENSION THERMAL NOISE REDUCTION

As part of a multistage seismic isolation system, the test masses of the Advanced LIGO interferometers are suspended from four 60-cm-long low-loss fused-silica fibers. The fibers have a circular cross section whose diameter varies to best cancel thermoelastic damping, to maintain low bounce-mode and high violin-mode frequencies and to ease handling and bonding to the test masses. Thermal noise from this suspension system dominates the total thermal noise below ~20 Hz (see Fig. 1). Fortunately, several low-risk methods are available for reducing suspension thermal noise [52].

The amplitude of suspension thermal noise scales as $1/l$, where l is the length of the suspension fibers. This scaling includes equal contributions from "dissipation dilution" and the improved isolation resulting from a downward shift in the horizontal resonant frequency. Further gains can be realized by refining the geometry of the fiber ends to improve dilution factors and by heat treatment of the fibers to reduce surface losses.

A longer suspension also presents lower thermal noise due to a reduction in the vertical (bounce-mode) resonant frequency [53], increasing the signal-to-noise ratio at very low frequencies. As more faithful waveform templates become available, this increase may help in estimating gravitational-wave source parameters that enter at low post-Newtonian order (e.g. chirp mass).

The improved rejection of seismic disturbances afforded by a longer suspension was not a significant factor in our study.

One recent investigation estimates that the above techniques can reduce the amplitude of suspension thermal noise by a factor of 2.5 [52]. In this work we conservatively assume a factor of two, realizing this improvement solely through increased suspension length and neglecting violin modes.

VIII. DISCUSSION

Each of these potential improvements to Advanced LIGO can offer a factor of two reduction in the corresponding noise term; although each noise term contributes significantly only at certain frequencies (see Fig. 1) and none is sufficiently dominant to effect more than a 30% change in BNS or BBH range (see Table I). A significant increase in inspiral range is only realized when improvements are implemented simultaneously.

Figure 3 conveys the relative importance of each potential upgrade—assuming all other improvements have already been made. For example, the quantum noise curves show BNS range as a function of measured high-frequency

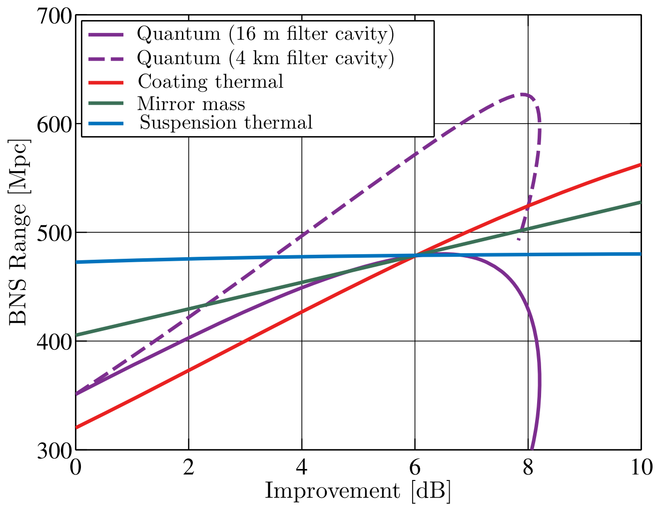

FIG. 3 (color online). BNS range as a function of improvement in the given quantities assuming all other upgrades have been implemented. For quantum noise, 'Improvement' describes the measured level of high-frequency squeezing; for mirror mass it expresses the mass increase factor and for thermal terms it captures the noise reduction factor. The four continuous curves intersect at the 6 dB point, where all noise terms have been reduced by a factor of two. In contrast to the baseline Advanced LIGO case, a longer filter cavity (dashed curve) proves significantly more effective in an upgraded interferometer.

squeezing for an interferometer in which coating thermal noise and suspension thermal noise have been reduced by a factor of two (or 6 dB) and the mass of the mirrors has been increased by a factor of two (all with respect to Advanced LIGO). Coating thermal noise reductions are shown to have the greatest effect on BNS range. Quantum noise improvements of up to 6 dB have comparable impact. Beyond this point BNS range does not increase monotonically with the level of detected squeezing due to currently achievable levels of technical noise, as in Advanced LIGO (see Fig. 2). However, in contrast, a 4 km long filter cavity is significantly more beneficial in an upgraded interferometer, since radiation pressure has become more influential at low frequencies. The maximum achievable BNS range is 20% higher with respect to a short filter cavity—bringing the maximum range to 580 Mpc for 6 dB of detected high-frequency squeezing.

Mitigating suspension thermal noise offers relatively modest gains in astrophysical output compared to the other approaches. By extension, this indicates that improvements in noise sources such as seismic noise and gravitational gradient noise, which are also prominent at very low frequencies, but less so than suspension thermal noise, will be even less effective.

For the BNS and BBH systems used to define our figures of merit, sensitivity around 100 Hz is of utmost importance. Yet the astrophysical impact of Advanced LIGO will likely not be limited to the detection of stellar-mass compact binaries. Indeed, several other sources are predicted to emit gravitational radiation detectable by ground-based interferometers. However, sensitivity to such systems may not be improved by all of the modifications discussed above. For example, many interesting sources emit gravitational waves in the 300–3000 Hz band, including core-collapse supernovae [54] and rapidly rotating neutron stars [55] (and references therein). In this frequency range, detector performance is limited entirely by quantum shot noise and is thus only improved by squeezed light injection.

It is currently anticipated that Advanced LIGO will undertake its first observing run (O1) in 2015, with subsequent runs of increasing sensitivity and duration in 2016–2017 (O2) and 2017–2018 (O3). Full design sensitivity should be achieved by 2019 [2]. We envisage that a squeezed light source will be installed after O2, with test mass and coating thermal noise upgrades being implemented following O3.

IX. CONCLUSIONS

Several improvements to Advanced LIGO will be possible over the next decade. Individually, these upgrades can be used to target particular frequency bands. In this work we have selected the most likely upgrades and, for the first time, evaluated how combinations of them perform. When implemented together, we find that the upgrades discussed herein offer a twofold increase in broadband sensitivity, enriching our astrophysical understanding and enhancing the importance of Advanced LIGO as a tool for multimessenger astronomy. The progression of upgrades to Advanced LIGO involving squeezed light, coating thermal noise reduction and heavier test masses offers a path for improvement which will increase the volume of the observable gravitational-wave universe by nearly an order of magnitude. While expected detection rates are currently very uncertain, even in the most pessimistic scenario these upgrades will take Advanced LIGO from observing a few events per year to observing a few events per month, a critical improvement as the era of gravitational-wave astronomy begins.

ACKNOWLEDGMENTS

The authors gratefully acknowledge the guidance of Rainer Weiss, Nergis Mavalvala, Rana Adhikari and David McClelland. They also thank Stefan Ballmer, Stefan Hild, Sheila Rowan and the other members of the LIGO Scientific Collaboration's Advanced Interferometer Configurations working group for useful discussions. LIGO was constructed by the California Institute of Technology and Massachusetts Institute of Technology with funding from the National Science Foundation and operates under Grant No. PHY-0757058. Advanced LIGO was built under award PHY-0823459.

[1] J. Degallaix *et al.* (The Virgo Collaboration), in *9th LISA Symposium, Paris, 2012*, Vol. 467 (Astronomical Society of the Pacific, San Francisco, 2013).
[2] The LIGO Scientific Collaboration, Classical Quantum Gravity **32**, 074001 (2015).
[3] Y. Aso, Y. Michimura, K. Somiya, M. Ando, O. Miyakawa, T. Sekiguchi, D. Tatsumi, and H. Yamamoto (The KAGRA Collaboration), Phys. Rev. D **88**, 043007 (2013).
[4] J. Abadie *et al.* (The LIGO Scientific Collaboration and the Virgo Collaboration), Classical Quantum Gravity **27**, 173001 (2010).
[5] B. Sathyaprakash *et al.*, Classical Quantum Gravity **29**, 124013 (2012).
[6] M. Punturo *et al.*, Classical Quantum Gravity **27**, 084007 (2010).
[7] T. G. F. Li, W. Del Pozzo, S. Vitale, C. Van Den Broeck, M. Agathos, J. Veitch, K. Grover, T. Sidery, R. Sturani, and A. Vecchio, Phys. Rev. D **85**, 082003 (2012).
[8] T. G. F. Li, W. Del Pozzo, S. Vitale, C. Van Den Broeck, M. Agathos, J. Veitch, K. Grover, T. Sidery, R. Sturani, and A. Vecchio, J. Phys. Conf. Ser. **363**, 012028 (2012).
[9] M. Agathos, W. Del Pozzo, T. G. F. Li, C. Van Den Broeck, J. Veitch, and S. Vitale, Phys. Rev. D **89**, 082001 (2014).
[10] W. Del Pozzo, T. G. F. Li, M. Agathos, C. Van Den Broeck, and S. Vitale, Phys. Rev. Lett. **111**, 071101 (2013).
[11] B. D. Lackey and L. Wade, arXiv:1410.8866 [Phys. Rev. D (to be published)].
[12] L. Wade, J. D. E. Creighton, E. Ochsner, B. D. Lackey, B. F. Farr, T. B. Littenberg, and V. Raymond, Phys. Rev. D **89**, 103012 (2014).
[13] L. Kreidberg, C. D. Bailyn, W. M. Farr, and V. Kalogera, Astrophys. J. **757**, 36 (2012).
[14] S. Nissanke, D. E. Holz, N. Dalal, S. A. Hughes, J. L. Sievers, and C. M. Hirata, arXiv:1307.2638.
[15] C. Messenger and J. Read, Phys. Rev. Lett. **108**, 091101 (2012).
[16] W. Del Pozzo, Phys. Rev. D **86**, 043011 (2012).
[17] M. Coleman Miller and E. J. M. Colbert, Int. J. Mod. Phys. D **D13**, 1 (2004).
[18] S. Gossan, J. Veitch, and B. S. Sathyaprakash, Phys. Rev. D **85**, 124056 (2012).
[19] R. X. Adhikari, Rev. Mod. Phys. **86**, 121 (2014).
[20] S. E. Dwyer, D. Sigg, S. Ballmer, L. Barsotti, N. Mavalvala, and M. Evans, arXiv:1410.0612.
[21] M. Punturo *et al.*, Classical Quantum Gravity **27**, 194002 (2010).
[22] C. M. Caves, Phys. Rev. Lett. **45**, 75 (1980).
[23] C. M. Caves, Phys. Rev. D **23**, 1693 (1981).
[24] Y. Levin, Phys. Lett. A **372**, 1941 (2008).
[25] P. R. Saulson, Phys. Rev. D **42**, 2437 (1990).
[26] C. Cutler, L. S. Finn, E. Poisson, and G. J. Sussman, Phys. Rev. D **47**, 1511 (1993).
[27] L. S. Finn, Phys. Rev. D **53**, 2878 (1996).
[28] B. Allen, W. G. Anderson, P. R. Brady, D. A. Brown, and J. D. E. Creighton, Phys. Rev. D **85**, 122006 (2012).
[29] S. S. Y. Chua, B. J. J. Slagmolen, D. A. Shaddock, and D. E. McClelland, Classical Quantum Gravity **31**, 183001 (2014).
[30] J. Abadie *et al.* (The LIGO Scientific Collaboration), Nat. Phys. **7**, 962 (2007).
[31] J. Aasi *et al.* (The LIGO Scientific Collaboration), Nat. Photonics **7**, 613 (2013).
[32] H. Grote, K. Danzmann, K. L. Dooley, R. Schnabel, J. Slutsky, and H. Vahlbruch, Phys. Rev. Lett. **110**, 181101 (2013).
[33] M. S. Stefszky, C. M. Mow-Lowry, S. S. Y. Chua, D. A. Shaddock, B. C. Buchler, H. Vahlbruch, A. Khalaidovski, R. Schnabel, P. K. Lam, and D. E. McClelland, Classical Quantum Gravity **29**, 145015 (2012).
[34] H. J. Kimble, Y. Levin, A. B. Matsko, K. S. Thorne, and S. P. Vyatchanin, Phys. Rev. D **65**, 022002 (2001).
[35] J. Harms, Y. Chen, S. Chelkowski, A. Franzen, H. Vahlbruch, K. Danzmann, and R. Schnabel, Phys. Rev. D **68**, 042001 (2003).
[36] P. Kwee, J. Miller, T. Isogai, L. Barsotti, and M. Evans, Phys. Rev. D **90**, 062006 (2014).
[37] R. Lynch, S. Vitale, L. Barsotti, M. Evans, and S. Dwyer, arXiv:1410.8503 [Phys. Rev. D (to be published)].
[38] M. Evans, L. Barsotti, P. Kwee, J. Harms, and H. Miao, Phys. Rev. D **88**, 022002 (2013).
[39] S. Chelkowski, H. Vahlbruch, B. Hage, A. Franzen, N. Lastzka, K. Danzmann, and R. Schnabel, Phys. Rev. A **71**, 013806 (2005).
[40] T. Isogai, J. Miller, P. Kwee, L. Barsotti, and M. Evans, Opt. Express **21**, 30114 (2013).
[41] G. M. Harry, A. M. Gretarsson, P. R. Saulson, S. E. Kittelberger, S. D. Penn, W. J. Startin, S. Rowan, M. M. Fejer, D. R. M. Crooks, G. Cagnoli, J. Hough, and N. Nakagawa, Classical Quantum Gravity **19**, 897 (2002).
[42] G. Harry, T. P. Bodiya, and R. DeSalvo, *Optical Coatings and Thermal Noise in Precision Measurement* (Cambridge University Press, Cambridge, 2012).
[43] G. M. Harry, M. R. Abernathy, A. E. Becerra-Toledo, H. Armandula, E. Black, K. Dooley, M. Eichenfield, C. Nwabugwu, A. Villar, D. R. M. Crooks, G. Cagnoli, J. Hough, C. R. How, I. MacLaren, P. Murray, S. Reid, S. Rowan, P. H. Sneddon, M. M. Fejer, R. Route, S. D. Penn, P. Ganau, J.-M. Mackowski, C. Michel, L. Pinard, and A. Remillieux, Classical Quantum Gravity **24**, 405 (2007).
[44] M. Evans, S. Ballmer, M. Fejer, P. Fritschel, G. Harry, and G. Ogin, Phys. Rev. D **78**, 102003 (2008).
[45] R. Flaminio, J. Franc, C. Michel, N. Morgado, L. Pinard, and B. Sassolas, Classical Quantum Gravity **27**, 084030 (2010).
[46] W. Yam, S. Gras, and M. Evans, Phys. Rev. D **91**, 042002 (2015).
[47] Most recently x has taken the value 0 for high index layers and 0.92 for low index layers [48]. Previously, 0.12 and 0.92 have been used [49].
[48] G. D. Cole, W. Zhang, M. J. Martin, J. Ye, and M. Aspelmeyer, Nat. Photonics **7**, 644 (2013).
[49] G. D. Cole, S. Gröblacher, K. Gugler, S. Gigan, and M. Aspelmeyer, Appl. Phys. Lett. **92**, 261108 (2008).
[50] J. A. Sidles and D. Sigg, Phys. Lett. A **354**, 167 (2006).
[51] K. L. Dooley, L. Barsotti, R. X. Adhikari, M. Evans, T. T. Fricke, P. Fritschel, V. Frolov, K. Kawabe, and N. Smith-Lefebvre, J. Opt. Soc. Am. A **30**, 2618 (2013).
[52] G. D. Hammond, A. V. Cumming, J. Hough, R. Kumar, K. Tokmakov, S. Reid, and S. Rowan, Classical Quantum Gravity **29**, 124009 (2012).
[53] Vertical motion couples to the longitudinal direction due to the curvature of the Earth.
[54] C. D. Ott, Classical Quantum Gravity **26**, 063001 (2009).
[55] The LIGO Scientific Collaboration and the Virgo Collaboration, Phys. Rev. D **91**, 022004 (2015).